THE JOURNAL OF BIOLOGICAL CHEMISTRY VOL. 288, NO. 8, pp. 5732–5742, February 22, 2013

Emodin Regulates Glucose Utilization by Activating AMP-activated Protein Kinase*[S]

Received for publication, December 1, 2012, and in revised form, January 5, 2013 Published, JBC Papers in Press, January 9, 2013, DOI 10.1074/jbc.M112.441477

Parkyong Song[‡], Jong Hyun Kim[‡], Jaewang Ghim[‡], Jong Hyuk Yoon[§], Areum Lee[‡], Yonghoon Kwon[‡], Hyunjung Hyun[¶], Hyo-Youl Moon[‖], Hueng-Sik Choi[**], Per-Olof Berggren[¶‡‡], Pann-Ghill Suh[‖], and Sung Ho Ryu[‡¶1]

From the [‡]Division of Molecular and Life Sciences, Pohang University of Science and Technology, Pohang, Kyungbuk 790-784, Republic of Korea, [§]NovaCell Technology Inc., Pohang, Kyungbuk 790-784, Republic of Korea, the [¶]Division of Integrative Biosciences and Biotechnology, Pohang University of Science and Technology, Pohang 790-784, Republic of Korea, the [‖]School of Nano-Biotechnology and Chemical Engineering, Ulsan National Institute of Science and Technology, Ulsan 689-805, Republic of Korea, the [**]Hormone Research Center, School of Biological Sciences and Technology, Chonnam National University, Gwangju, Republic of Korea, and the [‡‡]Rolf Luft Research Center for Diabetes and Endocrinology, Karolinska Institutet, SE-171 77 Stockholm, Sweden

Background: AMPK activation improves glucose tolerance and insulin sensitivity.
Results: Emodin increases glucose uptake in skeletal muscle and lowers blood glucose levels via AMPK activation.
Conclusion: Administration of emodin leads to increased glucose tolerance and insulin sensitivity *in vivo*.
Significance: Our results highlight the potential value of emodin as a drug for the treatment of diabetes.

AMP-activated protein kinase has been described as a key signaling protein that can regulate energy homeostasis. Here, we aimed to characterize novel AMP-activated kinase (AMPK)-activating compounds that have a much lower effective concentration than metformin. As a result, emodin, a natural anthraquinone derivative, was shown to stimulate AMPK activity in skeletal muscle and liver cells. Emodin enhanced GLUT4 translocation and [^{14}C]glucose uptake into the myotube in an AMPK-dependent manner. Also, emodin inhibited glucose production by suppressing the expression of key gluconeogenic genes, such as phosphoenolpyruvate carboxykinase and glucose-6-phosphatase, in hepatocytes. Furthermore, we found that emodin can activate AMPK by inhibiting mitochondrial respiratory complex I activity, leading to increased reactive oxygen species and Ca^{2+}/calmodulin-dependent protein kinase kinase activity. Finally, we confirmed that a single dose administration of emodin significantly decreased the fasting plasma glucose levels and improved glucose tolerance in C57Bl/6J mice. Increased insulin sensitivity was also confirmed after daily injection of emodin for 8 days using an insulin tolerance test and insulin-stimulated PI3K phosphorylation in wild type and high fat diet-induced diabetic mouse models. Our study suggests that emodin regulates glucose homeostasis *in vivo* by AMPK activation and that this may represent a novel therapeutic principle in the treatment of type 2 diabetic models.

AMPK[2] is a highly conserved mammalian serine/threonine protein kinase and acts as a master energy sensor that is responsible for regulating energy homeostasis (1, 2). These heterotrimeric enzymes are activated under cellular stress conditions such as starvation, exercise, oxidative damage, and hypoxia. Liver kinase B1 (LKB1) and Ca^{2+}/calmodulin-dependent protein kinase kinase (CaMKK) are two regulatory upstream kinases that stimulate AMPK phosphorylation (3). AMPK controls whole body energy homeostasis by regulating glucose and lipid metabolism in multiple peripheral tissues. For example, AMPK activation by 5-aminoimidazole-4-carboxamide-1-β-ribofuranoside stimulates glucose uptake via PI3K-independent GLUT4 translocation in skeletal muscle (4, 5) and inhibits hepatic glucose production (6).

Recently, many types of AMPK activators, including cytokines, drugs, and natural compounds, have been identified (3). Among them, metformin (1,1-dimethylbiguanide hydrochloride) and thiazolidinediones are widely used for the treatment of type 2 diabetes. The main function of metformin is to decrease blood glucose levels by inhibiting hepatic gluconeogenesis and increasing glucose uptake in skeletal muscle (7). Interestingly, the mitochondrial respiratory complex is the common target of metformin, which indirectly activates AMPK (8). Inhibition of complex I activity can cause changes in the cellular nucleotide ratio (9) and increase reactive oxygen species (10), which are important intermediates to increase AMPK activity. Despite their beneficial effects to glucose utilization, metformin must be administered at high concentrations, and they have adverse effects, such as gastrointestinal symptoms and relatively rare lactic acidosis *in vivo* (11). Furthermore,

* This work was supported by 21C Frontier Functional Proteomics Project Grant FPR08B1-160, World Class University Program Grant R31-2008-000-10105-0 funded by the Korean Ministry of Education, Science and Technology, Korea Health Technology R&D Project Grant A111345 from the Ministry of Health and Welfare, Republic of Korea, the Swedish Research Council, The Family Erling-Persson Foundation, and The Stichting af Jochnick Foundation.

[S] This article contains supplemental Figs. S1–S8.

[1] To whom correspondence should be addressed: POSTECH Biotech Center, San 31 Hyojadong, Pohang 790-784, Republic of Korea. Tel.: 82-54-279-2292; Fax: 82-54-279-0645; E-mail: sungho@postech.ac.kr.

[2] The abbreviations used are: AMPK, AMP-activated protein kinase; ACC, acetyl-CoA carboxylase; GLUT4, glucose transporter 4; PGC-1 α, peroxisome proliferator-activated receptor γ coactivator 1-α; ROS, reactive oxygen species; CaMKK, Ca^{2+}/calmodulin-dependent protein kinase kinase; 2-DOG, 2-deoxy-D-glucose; NAC, *N*-acetylcysteine; ITT, insulin tolerance test.

some human studies have shown that the glucose-lowering effects of metformin are secondary to reduction in hepatic gluconeogenesis (11–13). Thus, there is a growing demand to identify more effective AMPK activators, which have low dosage and affect various metabolic organs.

In this study, we screened a drug library to identify novel AMPK activators. As a result of this screening, emodin (1,3,8-trihydroxy-6-methylanthraquinone), a natural active compound in the herb *Rheum palmatum* L. was shown to stimulate the AMPK pathway. Some previous studies have suggested that emodin has an beneficial effect on energy metabolism, including adipocyte differentiation (14), anti-fibrotic effect on pancreatic fibrosis (15), and liver (16). However, validation of the molecular mechanism and the anti-diabetic effects of this compound has not been fully examined. Here, we show that emodin can increase glucose uptake in skeletal muscle via inhibition of mitochondrial complex I, which then leads to activation of AMPK. In addition, emodin inhibited hepatic gluconeogenesis through AMPK. Importantly, acute intravenous administration of emodin in both wild type and high fat diet-induced diabetic mice significantly decreased blood glucose levels associated with increased glucose utilization in skeletal muscle and liver. Based on the improved glucose metabolism and insulin sensitivity, this compound holds great promise for eventual use a therapeutic agent to treat type 2 diabetes.

EXPERIMENTAL PROCEDURES

Materials—5-Aminoimidazole-4-carboxamide-1-β-ribofuranoside was purchased from Toronto Research Chemical Inc. (Toronto, Ontario, Canada). Emodin, dichlorodihydrofluorescein diacetate, *o*-phenylenediamine, resveratrol, and metformin were purchased from Sigma, and 2-deoxy[^{14}C]glucose was from American Radiolabeled Chemicals Inc. Compound c, an AMPK inhibitor, and SB203580, a p38 MAPK inhibitor, were provided by Merck (RY 70-100).

Cell Culture—L6 myoblasts were grown in α-minimal essential medium, and mouse hepatoma Hepa1c1c7 cells were maintained in DMEM containing 10% fetal bovine serum (FBS), 50 units of penicillin/ml, and 50 μg of streptomycin/ml at 37 °C under humidified air atmosphere containing 5% CO_2. Differentiation of myoblast was induced in medium supplemented with 2% FBS within 7 days.

Immunoblotting—To prepare total cell lysates, myotube was washed with cold PBS and then lysed in cold lysis buffer (in mmol/liter: 40 HEPES, pH 7.5, 120 NaCl, 1 EDTA, 10 pyrophosphate, 10 glycerophosphate, 50 NaF, 1.5 Na_3VO_4, 1 PMSF, 5 $MgCl_2$, 0.5% Triton X-100, and protease inhibitor mixture). Transferred membrane was incubated with primary antibodies (1:1000) overnight at 4 °C. The following were used: p-AMPK-(Thr-172), ACC, p-Akt(Ser-473) (Cell Signaling Technology), AMPK (Upstate), p-ACC(Ser-79) (Millipore), phosphoenolpyruvate carboxykinase (Cayman), PGC1α (Abcam, UK), and monoclonal anti-Myc antibody (Millipore Corp., Billerica, MA).

AMPK Activity Assay—Cells were serum-fasted for 3 h and then treated with emodin for 5 min. After precipitation, AMPK activity was evaluated as incorporation of ^{32}P into a synthetic SAMS peptide in kinase reaction buffer (in mmol/liter: 40 HEPES, pH 7.5, 80 NaCl, 1 DTT, 0.2 AMP, 0.2 ATP, 5 $MgCl_2$, 0.1 SAMS, 0.25 [γ-^{32}P]ATP) at 30 °C for 20 min.

Determination of 2-Deoxy[^{14}C]glucose Uptake in Cells—2-Deoxyglucose uptake was determined as described previously (17). Briefly, differentiated L6 cells were serum-starved for 2 h prior to the assay. Cells were then washed twice with Krebs-Henseleit buffer and were stimulated with or without the indicated agents for 60 min. Glucose uptake was measured by incubation with 0.1 mCi/ml 2-deoxy[^{14}C]glucose at room temperature for 10 min.

Mitochondrial Complex I Activity—Cells were disrupted with nondenaturing detergent lauryl maltoside to maintain enzymatic activity and equilibrated with the indicated concentration of metformin and emodin for 10 min. Reaction was initiated by adding the reaction substrate NADH (500 μmol/liter) and ubiquinone-1 (50 μmol/liter). A decrease in 340 nm absorbance was recorded over 10 min using a UV spectrophotometer.

Fatty Acid Oxidation—Serum-fasted myotube was incubated with emodin for 2 h in oxidation media (0.1% lipid-free BSA, 100 μM [^{3}H]palmitate, vaporized for 30 min with N_2 gas to saturate palmitate). After oxidation, the rest of the free fatty acid was removed with 10% TCA precipitation. Supernatant in a capless microtube was vaporized in a scintillation tube with distilled water added at 50 °C for 12 h.

Mitochondrial Complex I Activity—Cells were disrupted with nondenaturing detergent lauryl maltoside to maintain enzymatic activity and equilibrated with the indicated concentration of metformin and emodin for 10 min. Reaction was initiated by adding the reaction substrate NADH (500 μmol/liter) and ubiquinone-1 (50 μmol/liter). A decrease in 340 nm absorbance was recorded over 10 min using a UV spectrophotometer.

Glucose Production Assay—Serum-fasted Hepa1c1c7 cells were pretreated with emodin at the indicated concentration for 10 min. After 18 h of stimulation with forskolin (10 μmol/liter)/dexamethasone (500 nmol/liter), the cells were treated with emodin for an additional 3 h. Glucose production was measured in glucose and phenol red-free DMEM, containing gluconeogenic substrate sodium lactate (20 mmol/liter) and sodium pyruvate (2 mmol/liter) for 8 h.

Quantitative PCR Analysis—Total RNA was isolated from hepatocyte and mouse liver tissue using the TRIzol reagent, and 3 μg of RNA was reverse-transcribed into cDNA. Quantitative real time PCR analysis was carried out using HotStart-IT SYBR® Green and Bio-Rad iCycler iQ. The sense and antisense primers used in PCR are listed in Table 1. The relative quantitation of mRNA was calculated by the comparative *Ct* method after normalization to ribosomal protein L32.

[Ca^{2+}]$_i$ Changes—[Ca^{2+}]$_i$ was measured using the fura-2 AM method. Briefly, cells were grown on coverslip and loaded with 1 μmol/liter fura-2 AM in loading buffer (in mmol/liter 125 NaCl, 5.9 KCl, 1.28 $CaCl_2$, 1.2 $MgCl_2$, 25 glucose, 0.1% BSA) for 30 min. During the experiment, cells were continuously drenched with the loading buffer. For [Ca^{2+}]$_i$ measurements after emodin treatment, fura-2 images were recorded using an OLYMPUS fluorescence microscope (DG4 light source), cap-

TABLE 1
Target gene primers sequences for quantitative-PCR analysis

Gene	Primer sequence	
	Forward	Reverse
G-6-Pase	TCCTGGGACAGACACACAAG	CAACTTTAATATACGCTATTGG
Pepck	CTTCTCTGCCAAGGTCATCC	TTTTGGGGATGGGCAC
Pgc-1α	ATACCGCAAAGAGCACGAGAAG	CTCAAGAGCAGCGAAAGCGTCACAG
MCP-1	AGGTGTCCCAAAGAAGCTGTA	ATGTCTGGACCCATTCCTTCT
IL6	AGGCTTAATTACACATGTTCTCTGG	TTATATCCAGTTTGGTAGCATCCAT
TNF-α	GATTTGCTATCTCATACCAGGAGAA	AAGTCTAAGTACTTGGGCAGATTGA
RPL 32	TTAAGCGAAACTGGCGGAAAC	TTGTTGCTCCCATAACCGATG

tured by a Hamamatsu's ImagEM electron multiplier CCD (EMCCD) camera, and analyzed using a MetaMorph program.

Animal Experiments—All experimental procedures involving animals were approved by the POTECH Animal Use and Care Committee. C57Bl/6J male mice (6–8 weeks old) were kept in a 12-h light/dark cycle with free access to water. To generate insulin resistance, mice received a high fat diet with 60% kcal fat for 10 weeks, and the body weight and blood glucose levels were investigated. Emodin was dissolved in a vehicle of 10% DMSO in saline/Tween 80. After emodin was injected intravenously, the fasting glucose levels were measured using a glucometer (Accu-Check Active; Roche Diagnostics) after the indicated time. Serum insulin levels were determined using insulin ELISA kits. For glucose tolerance test, overnight fasted mice were injected with emodin and metformin 30 min before intraperitoneal glucose injection (2 g/kg). Blood was collected from the tail vein at 15, 30, 60, and 120 min, and glucose levels were measured. For insulin tolerance test (ITT), fasted mice were injected intraperitoneally with 0.75 units/kg body weight, and blood glucose levels were measured at the indicated time point after injection. The liver and skeletal muscle were immediately frozen in liquid nitrogen and stored at −80 °C after sacrifice.

Pyruvate Tolerance Test—For the pyruvate tolerance test, mice received an intraperitoneal injection of sodium pyruvate (2 g/kg) dissolved in saline after 16 h of fasting.

Immunohistocytochemistry—Paraffin-embedded skeletal muscle was sectioned and incubated with F4/80 (ab6640, Abcam) and CD11b primary antibody (555386, BD Biosciences) for 4 h at RT. A biotinylated secondary antibody and HRP-streptavidin antibody with chromogen as a substrate were used for detection (Vectastain kit PK-6102, 6104; Burlingame, CA). The sections were counterstained in Harris' hematoxylin and eosin (H&E) staining.

Statistical Analysis—All data are expressed as means ± S.E. Statistical analysis between the two groups was performed by unpaired two-tailed Student's *t* test or one-way analysis of variance for multiple comparisons. *p* values of <0.05 were considered significant.

RESULTS

Emodin Activates AMPK Signaling Pathway in L6 Myotubes—To identify novel metabolic regulators, we carried out screening with the available drug library (supplemental Fig. 1*A*), and emodin (1,3,8-trihydroxy-6-methylanthraquinone) was identified to be a potent AMPK activator (supplemental Fig. 1, *C–G*). Similar to its activators of AMPK, emodin also elevated the phosphorylation level of AMPK and ACC in differentiated myotubes (Fig. 1*A*). AMPK activation by emodin occurred in a concentration- and time-dependent manner (Fig. 1, *B* and *C*). To further confirm the AMPK activation status, we performed a kinase assay with immunoprecipitated AMPK after emodin treatment. In these experiments, we observed emodin significantly enhanced AMPK activity (Fig. 1*D*). To compare the EC_{50} value of each known activator for AMPK phosphorylation, the effect of different concentrations of metformin, resveratrol, and emodin on AMPK activation was studied. As a result, 0.5 μM emodin was shown to reach half-effective concentration, which was much lower than metformin (~4 mM) and resveratrol (~50 μM) (Fig. 1*E*). Finally, there was no significant change in cell viability when cells were treated with emodin (supplemental Fig. 1*B*). These data indicate that emodin activates the AMPK pathway in myotubes at much lower concentrations than other naturally active compounds.

Effect of Emodin on Glucose Uptake in Myotubes—Next, we examined the effect of emodin on glucose uptake. In this analysis, we confirmed that emodin increased 2-deoxy[^{14}C]glucose uptake into myotubes in a concentration- and time-dependent manner (Fig. 2, *A* and *B*). To elucidate the mechanism behind this increase in glucose uptake, the level of surface GLUT4 was measured after emodin (3 μM) and metformin (10 mM) treatment by immunofluorescent microscopy. Because the Myc epitope is tagged at the extracellular region of GLUT4, translocation can be easily measured without any subcellular fractionation. Exposure of the Myc epitope at the plasma membrane was increased by emodin (Fig. 2*C*), which was in agreement with the glucose uptake results. We also used the *o*-phenylenediamine assay to accurately measure surface GLUT4, and we observed a 1.5-fold increase at 3 μM (Fig. 2*D*), which was comparable with the 10 mM metformin control.

To validate the effect of emodin on the insulin-mediated signaling pathway, we assessed the effect of co-treatment with emodin (3 μM) and insulin (25 nM) on AKT activation and glucose uptake. As shown in Fig. 2*E*, co-treatment did not interfere with the respective signaling pathways. Finally, emodin was shown to increase maximal insulin-stimulated glucose uptake (Fig. 2*F*). Taken together, our findings suggest that emodin increases GLUT4 translocation and glucose uptake, and co-treatment with emodin and insulin produced additive effects on glucose uptake through an independent pathway.

AMPK Mediates an Increase in Glucose Uptake by Emodin—To examine the importance of AMPK in emodin-induced glucose uptake, we used a selective AMPK chemical inhibitor and dominant negative AMPK α2 virus, which were shown to be the major isoform in skeletal muscle (18, 19). In these experiments,

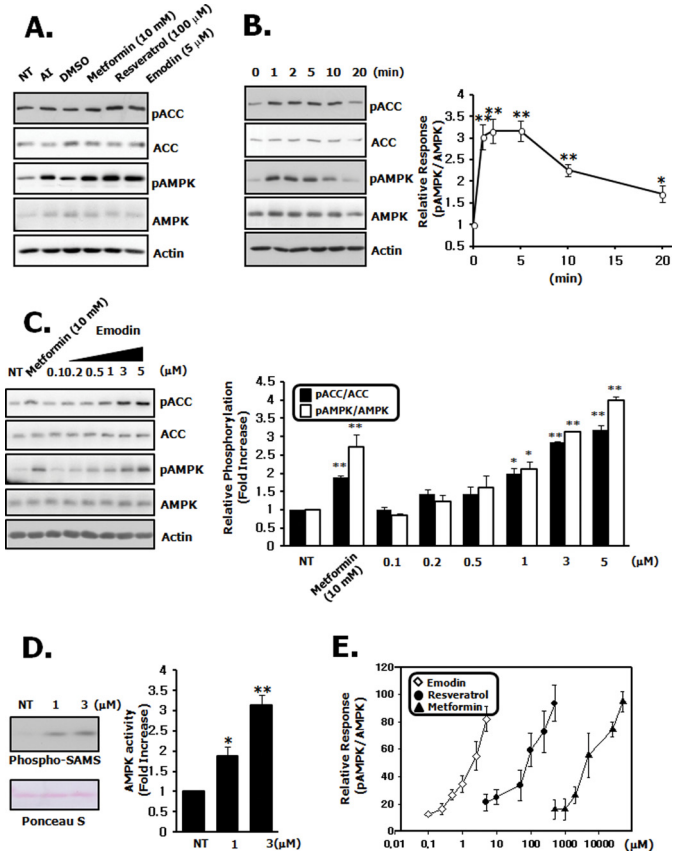

FIGURE 1. **Emodin stimulates AMPK pathway in L6 myotubes.** *A,* L6 myotubes were prepared as described under "Experimental Procedures." The cells were treated with 10 mM metformin for 2 h, 100 μM resveratrol for 1 h, and 5 μM emodin for 5 min. Cell lysates were analyzed by immunoblotting for phospho/total AMPK and ACC antibodies. *NT*, not treated; *AI*, positive control. *B,* L6 myotubes were stimulated with 3 μM emodin for an increasing amounts of time. *C,* L6 myotube was stimulated with an increasing concentration of emodin for 5 min. The levels of AMPK and ACC phosphorylation were quantified by densitometry and normalized to the total AMPK and ACC, respectively. *D,* AMPK activity was measured by SAMS peptide phosphorylation assay using immunoprecipitated AMPK. *E,* concentration-effect curve of various AMPK activators. The scales were selected so that the graphs were of roughly comparable height with the saturation point at 100. Data represent one of four independent experiments. Values are means ± S.E. *, $p < 0.05$, and **, $p < 0.01$ *versus* untreated cells.

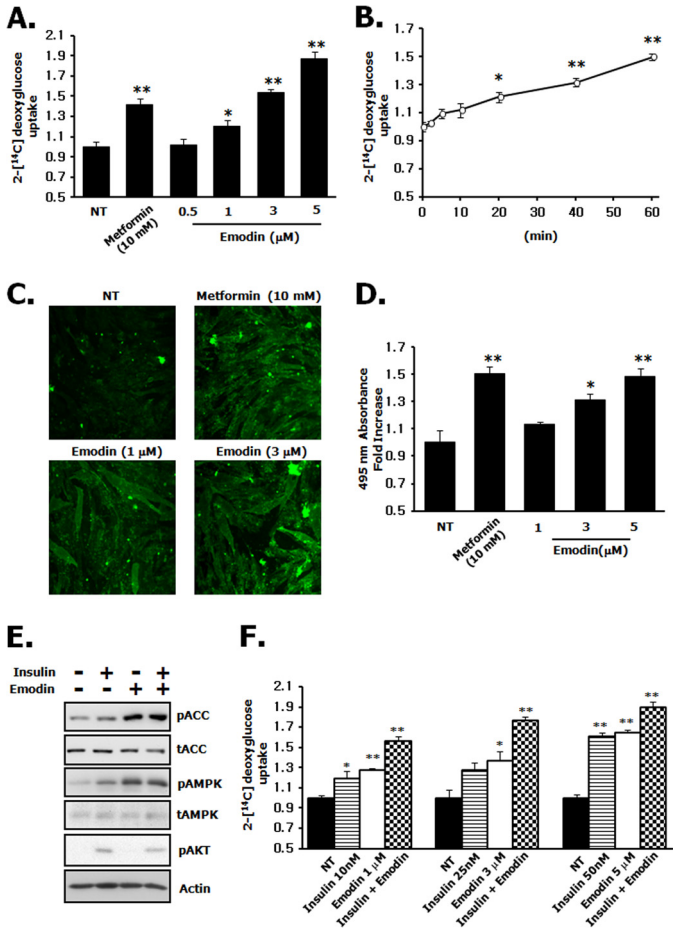

FIGURE 2. **Increase of GLUT4 translocation and glucose uptake in response to emodin.** *A,* L6 myotubes were equilibrated in glucose-free Krebs-Ringer buffer for 1 h and then incubated with the indicated concentrations of emodin for 1 h. [14C]2-DOG uptake was measured as described under "Experimental Procedures." *B,* L6 myotubes were incubated with 3 μM emodin for 0 to 1 h, and glucose uptake was measured. *C,* immunofluorescent detection of surface GLUT4 on confluent, quiescent L6 myotubes. The cells were treated with 3 μM emodin for 1 h, and surface GLUT4 levels were determined. NT, not treated with emodin. *D,* quantitative analysis of surface GLUT4. Exposure of GLUT4 was detected using the anti-Myc antibody and coupled to the *o*-phenylenediamine assay as described under "Experimental Procedures." *E,* co-treatment with 3 μM emodin and 25 nM insulin for 5 min. AMPK phosphorylation was quantified by densitometry and normalized to the total AMPK. Data represent one out of four independent experiments. *F,* [14C]2-DOG uptake was measured with emodin for 1 h and/or insulin for 10 min at the indicated concentration in L6 myotubes. Values are means ± S.E. of three independent experiments performed in triplicate. *, $p < 0.05$, and **, $p < 0.01$ *versus* untreated cells.

emodin-induced AMPK activation and increase in glucose uptake were completely blocked by compound C pretreatment without any effects on insulin-mediated AKT activation and glucose uptake (Fig. 3, *A* and *B*). These results indicate that the AMPK pathway is involved in emodin-mediated glucose uptake. Similar to the chemical inhibitor and knockdown results (supplemental Fig. 2*A*), infection with dominant negative AMPK α2 completely inhibited AMPK phosphorylation and glucose uptake induced by emodin, when compared with empty control virus (Fig. 3, *C* and *D*). These findings demonstrate that AMPK is a critical mediator of emodin-stimulated glucose uptake in skeletal muscle.

In addition to AMPK activation, it has also been suggested that insulin-mediated PI3K and p38 MAPK activation are involved in glucose uptake in skeletal muscle (20, 21). However, emodin did not activate AKT (Fig. 3*E*), and glucose uptake was not inhibited in cells pretreated with LY-294002, a PI3K inhibitor, or SB203580, a p38 MAPK inhibitor (Fig. 3*F*).

Intracellular ROS and Ca^{2+} Are Involved in Emodin-induced AMPK Activation and Glucose Uptake—Emodin could not activate AMPK directly (supplemental Fig. 3*A*). A previous report suggested that emodin can increase intracellular ROS levels in tumor cells (22). In addition, ROS has been shown to activate AMPK through an LKB1 and CaMKK-dependent pathway (23–25). Thus, we hypothesized that emodin-induced activation of AMPK was caused by ROS. First of all, emodin was shown to stimulate ROS production (Fig. 4*A* and supplemental Fig. 3*B*). Next, we examined changes in mitochondrial complex 1 activity, which is major target of metformin (8), to better understand the mechanism of ROS generation by emodin. As a result, emodin dose-dependently suppressed NADH oxidation, more effectively than metformin (Fig. 4*B*). As shown in Fig. 4, *C*

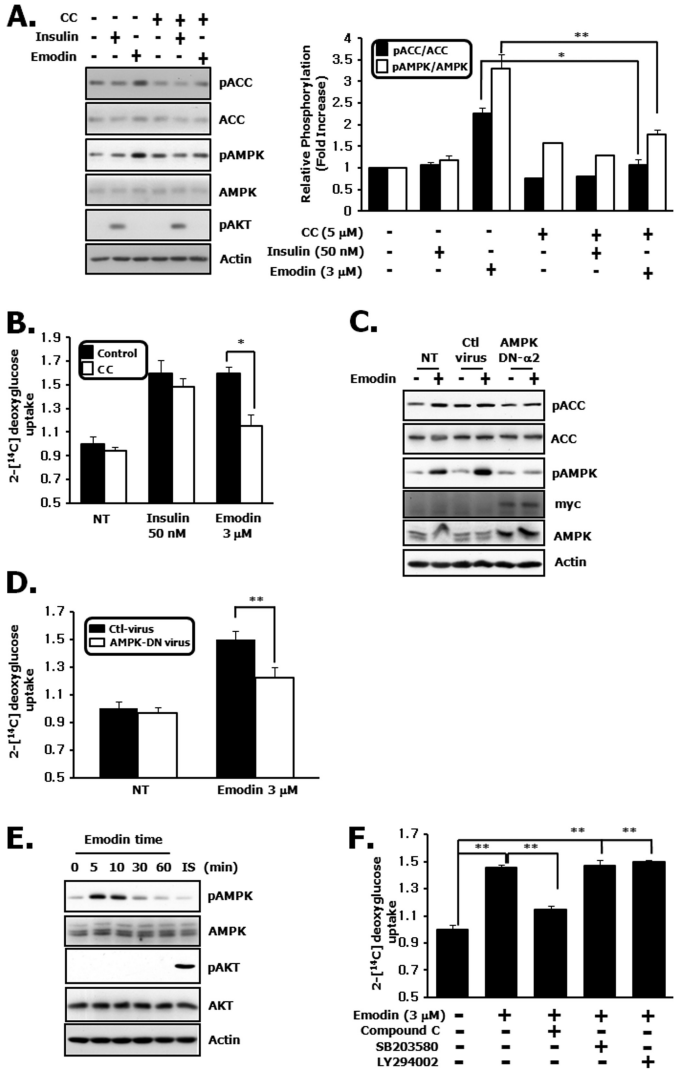

FIGURE 3. **Inhibition of AMPK blocks emodin induced glucose uptake.** *A,* after preincubation with 5 μM of compound c (*CC*) for 30 min, L6 myotubes were stimulated with 3 μM emodin or 25 nM insulin for 5 min. Data represent one of four independent experiments. *B,* cells were preincubated with compound c and stimulated at the indicated conditions. *NT,* not treated with emodin. [^{14}C]2-DOG uptake was measured for 10 min. *C,* L6 myotubes infected with either a mock or dominant negative-AMPK α2 adenovirus for 48 h were treated with or without emodin. DN-AMPK α2 expression was confirmed using the anti-Myc antibody. *NT,* not treated with any virus. *D,* [^{14}C]2-DOG uptake was measured with either a mock or DN-AMPK α2 adenovirus. *NT,* not treated with emodin. *E,* emodin effect is independent of AKT. Cells were stimulated for the indicated time period with emodin. The cell lysates were analyzed by immunoblotting for phosphor-/total AMPK and AKT antibody. Data represent one of four independent experiments. *F,* L6 myotubes were preincubated with AMPK inhibitor compound c, PI3K inhibitor LY 294002, and p38 MAPK inhibitor SB294002 for 1 h. [^{14}C]2-DOG uptake was measured for 10 min. Values are means ± S.E. of three independent experiments performed in triplicate. *, $p < 0.05$, and **, $p < 0.01$ compared between two groups as indicated.

and *D,* emodin induced AMPK phosphorylation, and *in vitro* kinase activity was largely inhibited by anti-oxidant *N*-acetylcysteine. In addition, the increase in glucose uptake was also blocked by *N*-acetylcysteine (Fig. 4*E*).

To verify which kind of upstream kinases were involved in the emodin-induced AMPK activation, we used HeLa cells, which do not express LKB1 protein. As shown in Fig. 4*F*, emodin-induced AMPK activation was also observed in HeLa cells, which means that emodin largely depends on the CaMKK. This hypothesis was further confirmed with a CaMKK inhibitor, STO-609. Pretreatment of myotubes and HeLa cells with STO-609 decreased AMPK phosphorylation (Fig. 4*F*). Similarly, emodin-induced glucose uptake was significantly attenuated by STO-609 (Fig. 4*G*). Finally, we examined change in cytoplasmic free Ca^{2+} concentration ($[Ca^{2+}]_i$), which is critical for CaMKK activation. As was observed for the signaling kinetics, an increased Fura ratio was detected immediately, going from 0.57 ± 0.005 to 1.02 ± 0.03 (Fig. 4*H*). Taken together, our findings indicate that emodin decreases mitochondrial complex I activity and stimulates AMPK through intracellular ROS-dependent Ca^{2+}-CaMKK pathway.

Emodin Affects Gluconeogenic Gene Expression and Hepatic Glucose Production—To examine the function of emodin on gluconeogenesis, we first checked the effect of emodin on the AMPK signaling pathway in a mouse hepatoma cell line. Exposure of mouse hepatocytes to emodin increased phosphorylation of AMPK and ACC within 5–30 min (Fig. 5*A* and supplemental Fig. 4*A*). To evaluate the effect of emodin on gluconeogenesis in hepatocytes, we measured glucose production with or without emodin. As shown Fig. 5*B* and supplemen- tal Fig. 4*B*, we found that emodin suppressed the increased glucose levels caused by forskolin/dexamethasone in a concentration-dependent manner. Next, we examined the effects of emodin on the expression of gluconeogenic genes. As shown in Fig. 5*C* and supplemental Fig. 4*C*, increased transcript levels of important gluconeogenic genes were largely suppressed by emodin treatment. Finally, suppression of glucose production was also recovered by AMPK inhibition (Fig. 5*D*). These results show that emodin can suppress hepatic glucose production and gluconeogenic genes via stimulating AMPK activity.

Emodin Decreases Blood Glucose Concentration in Wild Type Mice—To investigate glucose homeostasis and insulin sensitivity after emodin treatment *in vivo*, we first examined AMPK phosphorylation in skeletal muscle and liver after intravenous injection of emodin (1 mg/kg). When compared with vehicle, emodin induced a significant increase in AMPK phosphorylation in both tissues, which was consistent with the *in vitro* results (Fig. 6*A*). More importantly, a single intravenous injection of emodin (1 mg/kg) significantly decreased fasting blood glucose levels in wild type mice at each indicated time point (Fig. 6*B*). After 3 h, emodin decreased blood glucose levels by 42%, from 185 ± 9 mg/dl (injection start point) to 106 ± 6 mg/dl, whereas metformin (125 mg/kg) only decreased blood glucose levels by 28%, from 168 ± 12 to 121 ± 6 mg/dl. The decrease caused by administration of vehicle was 15%, from 176 ± 14 to 149 ± 10 mg/dl. There was no change in serum insulin levels between vehicle and emodin injection group (1.33 ± 0.1 *versus* 1.04 ± 0.2 ng/ml) (Fig. 6*C*). These results strongly suggest that the glucose lowering effects of emodin are mediated by AMPK-dependent and PI3K-independent phenomena.

To further confirm the AMPK dependence *in vivo*, we examined the glucose-lowering effect of emodin with or without compound c. In a previous report and our result (supplemental Fig. 5), i.v. injection of compound c was shown to eliminate phosphorylation of AMPK and ACC (26). In compound

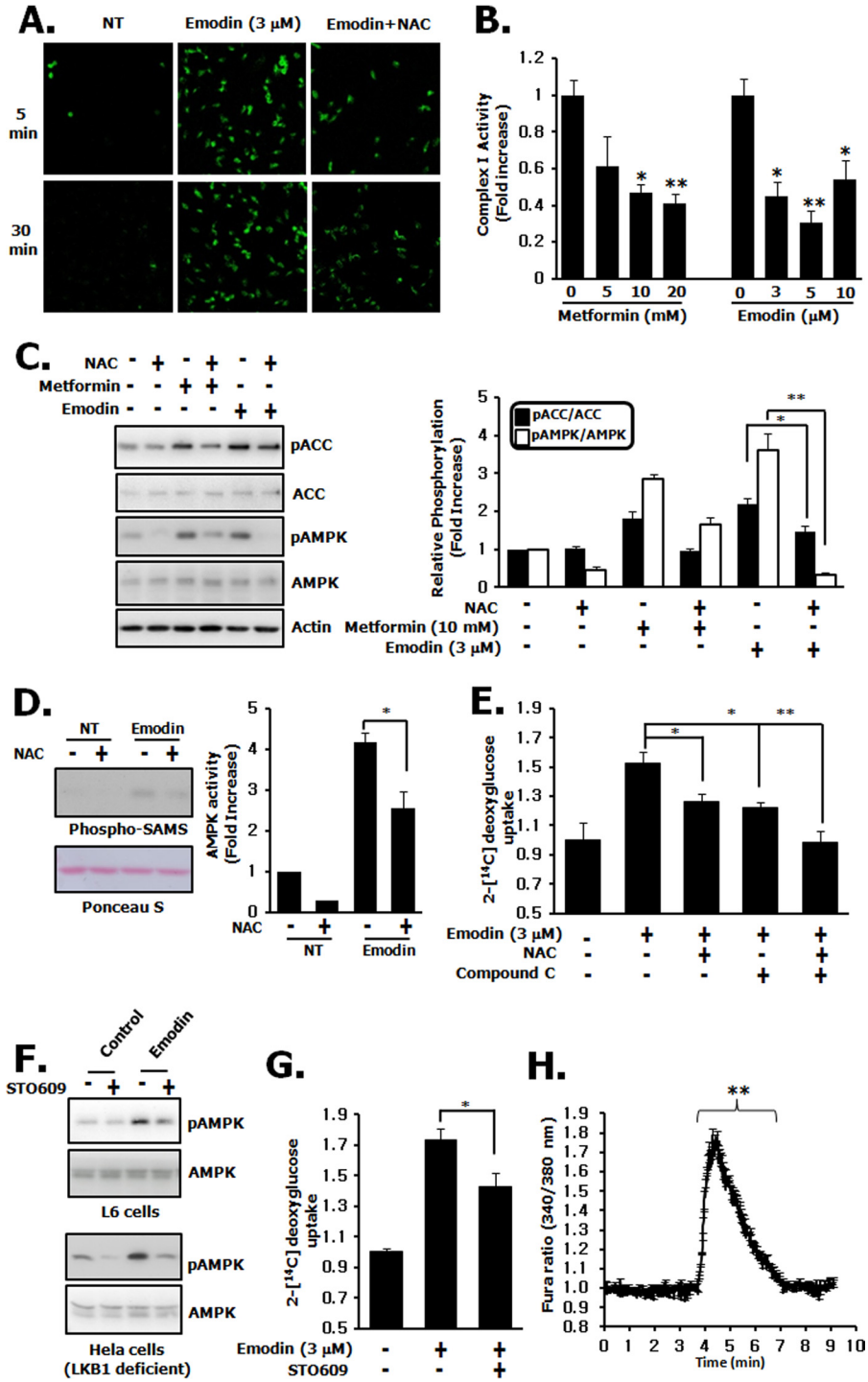

FIGURE 4. **AMPK activation and stimulation of glucose uptake is ROS-CaMKK-dependent.** *A,* intracellular ROS generation by emodin. Cells were serum-starved for 3 h and incubated with emodin for the indicated times in the presence or absence NAC. ROS levels were measured using dihydrodichlorofluorescein diacetate. Increased ROS generation was visualized by fluorescence microcopy. *NT*, not treated with emodin. *B,* effects of metformin and emodin on mitochondrial complex I activity were measured after 10 min at the indicated concentrations. The relative activity was expressed as a decrease in absorbance at 340 nm. *C,* after preincubating with NAC for 30 min, L6 myotubes were stimulated with 10 mM metformin for 1 h and 3 μM emodin for 5 min. The cell lysates were analyzed for phosphorylation-specific antibodies. Data represent one of four independent experiments. *D,* AMPK activity was measured by SAMS peptide phosphorylation assay using immunoprecipitated AMPK and NAC. *E,* [^{14}C]2-DOG uptake was measured for 10 min in the presence of compound c or NAC. *F,* L6 myotubes and HeLa cells were stimulated with 3 μM emodin for 5 min with or without CaMKK inhibitor STO-609. The cell lysates were analyzed by immunoblotting, using phosphorylation-specific antibodies. *G,* L6 myotube was preincubated with CaMKK inhibitor STO-609 for 30 min and then treated with 3 μM emodin. [^{14}C]2-DOG uptake was measured for 10 min. *H,* cells were loaded with Fura2-AM for 30 min and treated with emodin. Response of single cell was recorded using a fluorescence microscope, captured by an EMCCD camera. Values are means ± S.E. of three independent experiments performed in triplicate. For the $[Ca^{2+}]_i$ measurements, 69 cells were used. *, $p < 0.05$, and **, $p < 0.01$ compared between two groups as indicated.

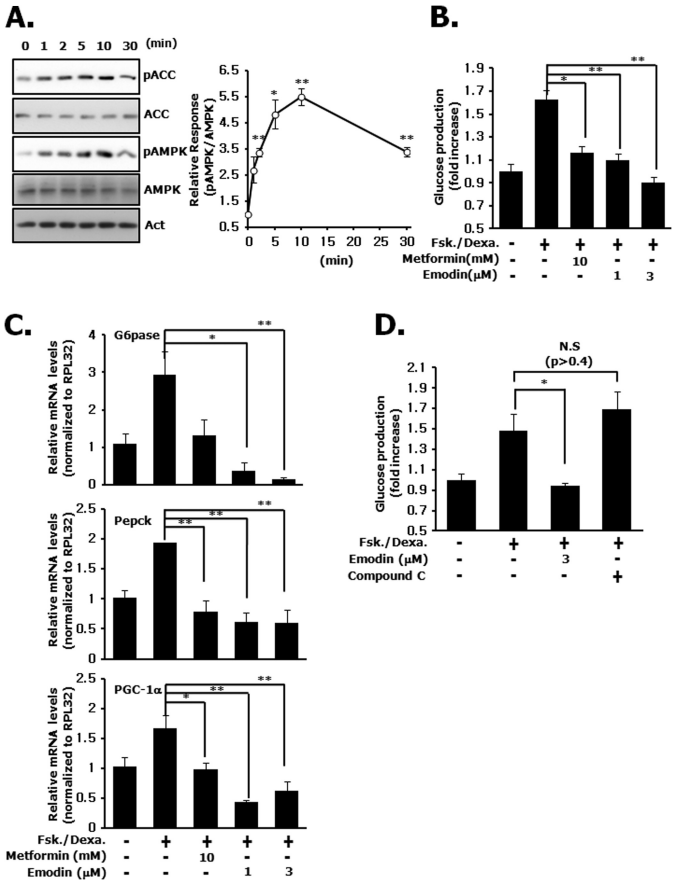

FIGURE 5. **Emodin phosphorylates AMPK and suppresses gluconeogenesis in hepatocyte.** *A,* Hepa1c1c7 cells were fasted for 12 h and treated with 3 μM emodin for various time points. AMPK phosphorylation was quantified by densitometry and normalized to the total AMPK. Data represent one of four independent experiments. *ACT*, actin. *B,* serum-fasted cells were treated with emodin for 10 min and then stimulated with forskolin/dexamethasone (*Fsk/Dexa*) for an additional 18 h. Glucose production was measured for 8 h as described under "Experimental Procedures." *C,* relative changes in the gluconeogenic mRNA levels. *D,* glucose production was measured with or without compound c. Values are means ± S.E. of three independent experiments performed in triplicate. *, $p < 0.05$, and **, $p < 0.01$ compared between two groups as indicated. *G6Pase*, glucose-6-phosphatase; *N.S.,* not significant.

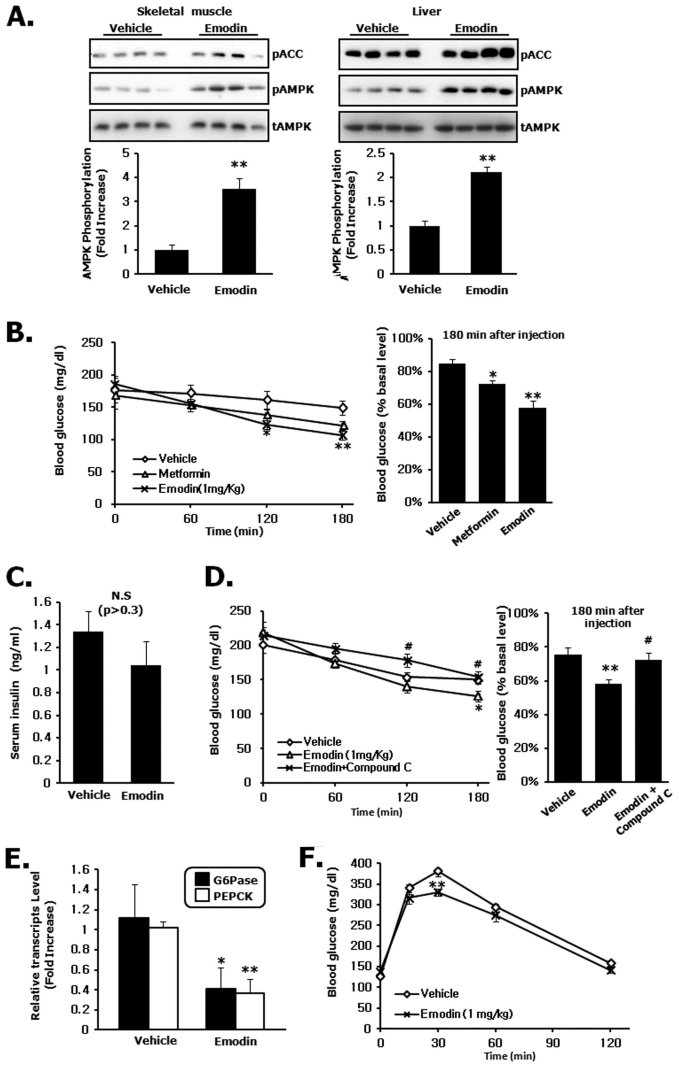

FIGURE 6. **Emodin activates AMPK and decreases fasting glucose levels in wild type mice.** *A,* AMPK and ACC phosphorylation in skeletal muscle and liver of wild type C57Bl/6J mice was evaluated after a single intravenous injection of emodin. *B,* acute fasting glucose-lowering effect of emodin. Eight-week-old male mice were intravenously treated with metformin and emodin at the indicated dose. Blood glucose levels were measured every 60 min. *C,* serum insulin levels 3 h after intravenous injection of vehicle and emodin. *D,* effect of AMPK inhibitor compound c in the emodin-injected groups. Mice were pretreated with compound c (2 mg/kg) for 30 min and intravenously treated with the vehicle and emodin. *E,* mRNA level of hepatic gluconeogenic genes in the liver were measured in mice that were intravenously treated with vehicle and emodin. *F,* glucose tolerance was determined 30 min after injection of 1 mg/kg emodin. Glucose (2 g/kg) was injected intraperitoneally. Results are the means ± S.E. of six mice per group ($n = 6$). Statistical analysis conducted on fasting glucose lowering was performed using one-way analysis of variance and Tukey's multiple comparison test. *, $p < 0.05$, and **, $p < 0.01$ *versus* vehicle treatment. #, $p < 0.05$ *versus* emodin groups. *G6Pase*, glucose-6-phosphatase; *N.S.,* not significant.

c-treated mice, the blood glucose levels were much higher than those in the emodin alone-treated group at all time points (Fig. 6*D*), and attenuation of the glucose-lowering effect of compound c was profound at 2 h (decreased by 36% blood glucose level from 218 ± 16 to 140 ± 9 mg/dl with emodin and 17% from 214 ± 12 to 178 ± 11 mg/dl with compound c co-injection). Furthermore, emodin suppressed phosphoenolpyruvate carboxykinase and glucose-6-phosphatase gene expression (Fig. 6*E*). Finally, administration of emodin significantly reduced blood glucose levels in a glucose tolerance test (Fig. 6*F*).

Emodin Stimulates Glucose Utilization and Increases Insulin Sensitivity in High Fat-induced Diabetic Mice—We also evaluated the acute and chronic glucose-lowering effect of emodin in type 2 diabetic mouse models. Consistent with the wild type results, phosphorylation of AMPK in skeletal muscle was also significantly increased after single intravenous injection of emodin (3 mg/kg) (Fig. 7*A*). In addition, these effects correlated with a decrease in fasting glucose levels, the decrease being 36%, from 241 ± 47 mg/dl (injection start point) to 154 ± 28 mg/dl (Fig. 7*B*). More importantly, compound c significantly inhibited the glucose-lowering effect caused by emodin, which means that the acute effect of emodin on blood glucose levels is largely dependent on AMPK activity. During the glucose tolerance tests, impaired glucose tolerance in high fat diet-induced obese mice was markedly improved in the emodin-injected group, and the improvement was much more distinct than that observed in wild type mice (Fig. 7*C*). To examine insulin sensitivity in chronic emodin-administered mice, we investigated

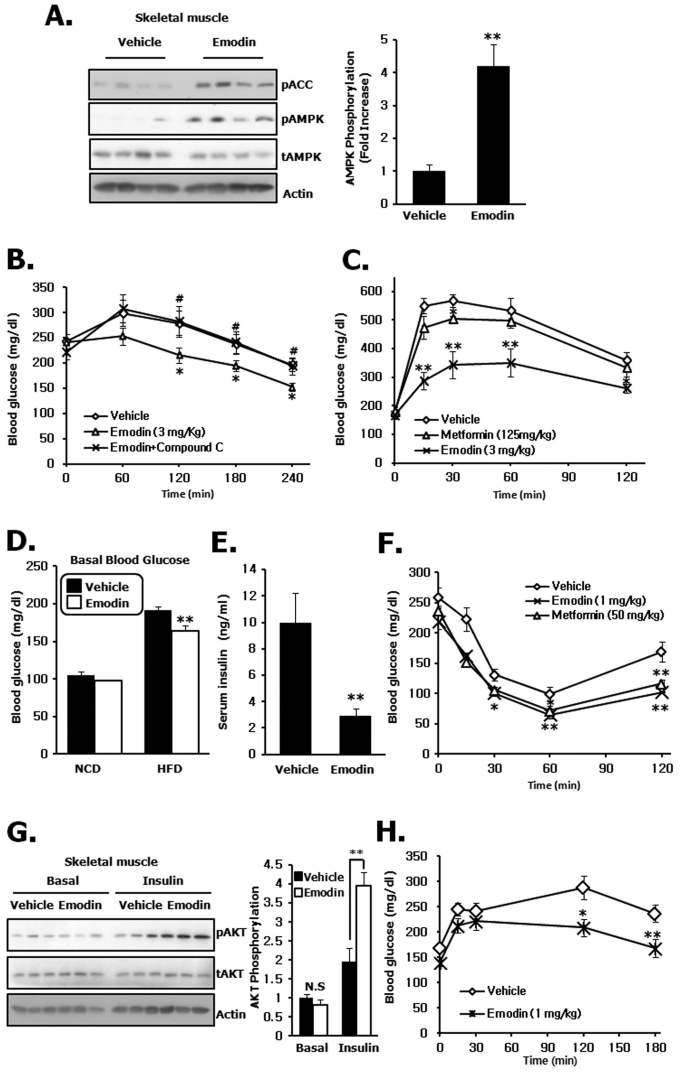

FIGURE 7. **Emodin improves glucose tolerance and insulin sensitivity in high fat induced diabetic mice.** *A,* AMPK and ACC phosphorylation in skeletal muscle of high fat diet-induced C57Bl/6J obese mice after a single intravenous injection of emodin at the indicated dose. *B,* effect of AMPK inhibitor compound c in emodin-injected groups. Mice were pretreated with compound c (2 mg/kg) for 30 min and injected intravenously with the vehicle and emodin. *C,* blood glucose levels were measured after intraperitoneal glucose injection (2 g/kg) in single i.v. administration of emodin. *D* and *E,* basal glucose levels and fed insulin levels were measured after 8 days injection of emodin. *NCD,* normal chow diet; *HFD,* high fat diet. *F,* ITT after daily i.v. injection of emodin and metformin for 8 days. Blood glucose levels were measured after intraperitoneal insulin injection (0.75 units/kg). *G,* representative AKT phosphorylation in skeletal muscle under basal conditions was compared with that after insulin treatment in mice subjected to emodin i.v. injection for 8 days. *H,* pyruvate tolerance test after 8 days of injection of emodin. Results are the means ± S.E. of nine mice per group ($n = 9$). For the ITT, five mice per group ($n = 5$). One-way analysis of variance, Tukey's multiple comparison test was performed at fasting glucose lowering and glucose tolerance test. *, $p < 0.05$, and **, $p < 0.01$ *versus* vehicle treatment; #, $p < 0.01$ *versus* emodin groups. *N.S.,* not significant.

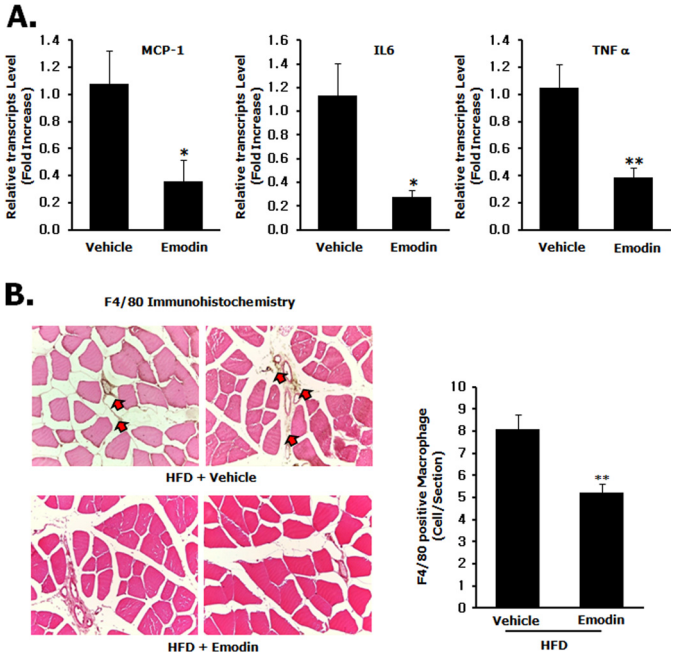

FIGURE 8. **Decreased muscle pro-inflammatory cytokines and macrophages.** *A,* relative mRNA levels of inflammatory cytokines in skeletal muscle were measured. *B,* representative F4/80 staining of macrophages in skeletal muscle. Muscle sections of vehicle or emodin-treated high fat diet (*HFD*)-induced obese mice were stained for the general macrophage marker F4/80 with magnification ×40. Magnification ×20 was used for the quantification ($n = 10$). *, $p < 0.05$, and **, $p < 0.01$ *versus* vehicle treatment.

insulin tolerance after daily injection of emodin for 8 days. During this period, there was no change in food intake and body weight (supplemental Fig. 6, *A* and *B*). When we treated emodin for 8 days, both basal blood glucose levels (Fig. 7*D*) and fed insulin levels (Fig. 7*E*) were significantly decreased. Furthermore, insulin-mediated glucose-lowering effects in ITT were more obvious than the vehicle group (Fig. 7*F*), and AKT phosphorylation by insulin was significantly increased in emodin-injected mice (Fig. 7*G*). Finally, increased blood glucose levels were largely attenuated in emodin-treated mice in a pyruvate tolerance test, indicating reduced gluconeogenesis in liver (Fig. 7*H*). Together, our results suggest that emodin activates AMPK *in vivo*, which is responsible for increased glucose tolerance and insulin sensitivity in multiple peripheral tissues.

Diet-induced Inflammatory Cytokines and Macrophages Are Attenuated after Emodin Administration—It has been demonstrated that inflammatory cytokines in skeletal muscle and adipose tissue are elevated in obesity (27). To elucidate the effect of emodin on muscle inflammatory cytokine and macrophage levels, we measured transcript levels of pro-inflammatory cytokine after treatment of emodin in high fat diet-induced obese mice. Fig. 8*A* and supplemental Fig. 7 indicate that the cytokine transcript levels were largely inhibited. Furthermore, infiltration of F4/80-positive macrophages was also suppressed by chronic treatment of emodin (Fig. 8*B*). These results suggest that emodin decreases diet-induced inflammation status in the skeletal muscle.

DISCUSSION

It has been demonstrated that emodin suppresses cell growth and proliferation in many types of tumor cells (22, 28, 29), and it inhibits inflammations in vascular endothelial cells (30, 31). In this study, we found that emodin activates AMPK by modulating mitochondrial complex I activity. Through inhibiting complex I, emodin increases cellular ROS and Ca^{2+} influx, which are well known conditions for AMPK activation. Importantly, the effect of emodin was much more potent than that of metformin and extended to muscle and liver. As an anti-tumor agent, the required effective concentration of emodin *in vivo* is

relatively high, and it inhibits only some types of tumors but not nontumor cells (22, 28). The emodin concentrations (up to 5 μM) used in this study does not cause cell death or apoptosis as measured using the 3-(4,5-dimethylthiazol-2-yl)-2,5-diphenyltetrazolium bromide assay. In addition, a very recent paper showed that exposure to nearly 800 mg/kg emodin for 14 weeks through the diet did not show any developmental and testicular toxicity in wild type mice (32, 33). Hence, the low concentration range that we have used is reasonable with regard to a potential therapeutic treatment regimen for type 2 diabetes.

Mitochondrial complex I is the rate-limiting step of the electron transport chain. In addition to cellular respiration, the importance of complex I as a diabetic target has been suggested. Metformin directly inhibits complex I, which leads to an increase in AMPK activity and insulin sensitivity (8, 34). We have also observed that emodin decreased NADH conversion to NAD^+, which means complex I activity was inhibited. This, in combination with the relationship between AMPK and mitochondria, suggests that emodin increases AMPK activity by modulating mitochondrial metabolism in skeletal muscle. One possibility is the competitive inhibition between emodin and ubiquinone, a membrane-embedded electron carrier (35). Because emodin (1,3,8-trihydroxy-6-methylanthraquinone) also belongs to the quinone family, it is possible that they have a common binding site in the complex I subunit. Therefore, it would be worth examining if the binding domain of ubiquinone overlaps with that of emodin.

A recent study demonstrated that chronic treatment with emodin lowered body weight in the diet-induced obese mouse by suppressing 11β-hydroxysteroid dehydrogenase type 1 (11-HSD1) activity in liver and adipose tissue (36). 11-HSD1 is an NADPH-dependent enzyme that is related to obesity and insulin resistance via the glucocorticoid signal (37). This study suggested that reduced food intake, by inhibition of the orexigenic glucocorticoid signal, may partly contribute to body weight loss. Although reduced fat mass and serum lipid contents through the inhibitory function on 11-HSD1 in liver and adipocyte tissue are important *in vivo*, emodin-induced AMPK activation in skeletal muscle may be another major anti-diabetic mechanism. Skeletal muscle constitutes ~40% of body mass and is an essential tissue responsible for 75% of the whole body glucose uptake to exert glucose lowering (38). Indeed, in our study, AMPK inhibitor compound c largely attenuated glucose uptake in skeletal muscle cells, resulting in much less effective glucose lowering in a mouse model. In addition, emodin-induced AMPK activation can contribute to weight loss, because AMPK is known to increase fatty acid oxidation (39, 40) and mitochondrial biogenesis (19), which protects against obesity (2). The data provided in this study, where AMPK was shown to increase fatty acid oxidation and related genes, support this hypothesis (supplemental Fig. 8, *A* and *B*). In fact, a very recent paper also reports that emodin increases AMPK and ACC in hepatocytes and adipose tissues of high fat diet-fed rats and improves dyslipidemia after 8 weeks of treatment (41, 42).

In contrast to chronic exposures, many reports have suggested that modest ROS generation represents a favorable condition for glucose utilization (43). For example, ROS can decrease protein phosphatase activity, such as PTP1B (44) and PTEN (45). In addition, ROS also stimulates AMPK activity in many peripheral tissues (25, 46, 47), and it is well known that ROS generated during exercise and muscle contraction accelerates glucose uptake in skeletal muscle through AMPK (48, 49). Metformin and epigallocatechin-3-gallate suppress hepatic gluconeogenesis by ROS-mediated AMPK activation in the liver (50). By using genetic models, many groups have demonstrated the acute requirement of ROS for AMPK activation, which has many beneficial metabolic effects (47, 51, 52). Based on the significant inhibition of AMPK and glucose uptake by NAC, we suggest that ROS generation by emodin plays an important role in the activation AMPK. Of course, it is still possible that other mechanisms are involved in the induction of AMPK activity. Mitochondrial uncoupling proteins function with ROS to produce heat without ATP generation, and we also observed a small but statistically significant decrease in ATP content (Table 2). However, given the AMPK phosphorylation in LKB1(−/−) cells, AMP/ATP ratio changes may take small charge of emodin-induced AMPK activation, because LKB1 is a critical upstream kinase to activate AMPK under AMP-enriched conditions. When we consider the importance of LKB1 in actions of metformin (53), this difference would be a clue for explaining distinct kinetics and *in vivo* potency between emodin and metformin. Furthermore, some previous results and our experimental results suggest that the liver is the main target tissue of metformin to show a glucose-lowering effect (11, 13). So, when compared with metformin, emodin does not have tissue specificity and has a comparative advantage regarding this aspect.

TABLE 2

Adenine nucleotide concentrations after emodin treatment

Effect of emodin on the intracellular AMP/ATP contents is shown. Cell lysates were extracted with a perchloric acid and analyzed using HPLC. Values are means ±S.E. of two independent experiments performed in triplicate.

Treatment	AMP	ATP	AMP/ATP ratio
	nmol/mg	*nmol/mg*	
Not treated	0.90 ± 0.09	34.4 ± 1.96	0.026 ± 0.001
Emodin (3 μM)	1.13 ± 0.31	29.2 ± 2.44[a]	0.040 ± 0.01

[a] $p < 0.05$ *versus* untreated cells.

Blood glucose concentration is mainly regulated by glucose uptake in skeletal muscle and glucose production in liver. To determine whether emodin can also activate AMPK and decrease blood glucose *in vivo*, we carried out a single and prolonged intravenous administration of emodin in wild type and high fat diet-induced obese mice. Remarkably, a single injection of emodin sufficiently lowered fasting glucose levels within 3 h in both *in vivo* models, and this effect was much more potent than the effect observed in the metformin groups. Because there was no change in serum insulin levels between vehicle and emodin administration, the AMPK pathway is likely the main mechanism by which emodin regulates blood glucose levels. Also, we observed that emodin was able to improve glucose tolerance both in wild type and high fat diet-induced diabetic mice, and chronic treatment increased insulin sensitivity.

In summary, we show that emodin improves glucose utilization in wild type and diabetic mouse models. The main mechanisms of these glucose-lowering effects are stimulation of glu-

cose uptake in skeletal muscle and suppression of hepatic gluconeogenesis via AMPK phosphorylation. Furthermore, AMPK activation is mediated by inhibiting the enzymatic activity of complex I of the respiratory chain. Hence, we have identified a new mechanism whereby emodin lowers plasma glucose levels, which may have interesting implications for the treatment of type 2 diabetes.

Acknowledgments—We thank Dr. Joohun Ha and colleagues (Kyung Hee University College of Medicine, Republic of Korea) for the generous gift of adenovirus. We are grateful to Dr. Amira Klip (Hospital for Sick Children, Toronto, Canada) for kindly providing the L6 GLUT4myc myoblast.

REFERENCES

1. Hardie, D. G. (2004) The AMP-activated protein kinase pathway–new players upstream and downstream. *J. Cell Sci.* **117,** 5479–5487
2. Kahn, B. B., Alquier, T., Carling, D., and Hardie, D. G. (2005) AMP-activated protein kinase: ancient energy gauge provides clues to modern understanding of metabolism. *Cell Metab.* **1,** 15–25
3. Hardie, D. G. (2007) AMP-activated/SNF1 protein kinases. Conserved guardians of cellular energy. *Nat. Rev. Mol. Cell Biol.* **8,** 774–785
4. Koistinen, H. A., Galuska, D., Chibalin, A. V., Yang, J., Zierath, J. R., Holman, G. D., and Wallberg-Henriksson, H. (2003) 5-Amino-imidazole carboxamide riboside increases glucose transport and cell-surface GLUT4 content in skeletal muscle from subjects with type 2 diabetes. *Diabetes* **52,** 1066–1072
5. Musi, N., Hayashi, T., Fujii, N., Hirshman, M. F., Witters, L. A., and Goodyear, L. J. (2001) AMP-activated protein kinase activity and glucose uptake in rat skeletal muscle. *Am. J. Physiol. Endocrinol. Metab.* **280,** E677–E684
6. Lochhead, P. A., Salt, I. P., Walker, K. S., Hardie, D. G., and Sutherland, C. (2000) 5-Aminoimidazole-4-carboxamide riboside mimics the effects of insulin on the expression of the 2 key gluconeogenic genes PEPCK and glucose-6-phosphatase. *Diabetes* **49,** 896–903
7. Musi, N., Hirshman, M. F., Nygren, J., Svanfeldt, M., Bavenholm, P., Rooyackers, O., Zhou, G., Williamson, J. M., Ljunqvist, O., Efendic, S., Moller, D. E., Thorell, A., and Goodyear, L. J. (2002) Metformin increases AMP-activated protein kinase activity in skeletal muscle of subjects with type 2 diabetes. *Diabetes* **51,** 2074–2081
8. Brunmair, B., Staniek, K., Gras, F., Scharf, N., Althaym, A., Clara, R., Roden, M., Gnaiger, E., Nohl, H., Waldhäusl, W., and Fürnsinn, C. (2004) Thiazolidinediones, like metformin, inhibit respiratory complex I. A common mechanism contributing to their antidiabetic actions? *Diabetes* **53,** 1052–1059
9. Hawley, S. A., Ross, F. A., Chevtzoff, C., Green, K. A., Evans, A., Fogarty, S., Towler, M. C., Brown, L. J., Ogunbayo, O. A., Evans, A. M., and Hardie, D. G. (2010) Use of cells expressing γ subunit variants to identify diverse mechanisms of AMPK activation. *Cell Metab.* **11,** 554–565
10. Lambert, A. J., and Brand, M. D. (2004) Inhibitors of the quinone-binding site allow rapid superoxide production from mitochondrial NADH: ubiquinone oxidoreductase (complex I). *J. Biol. Chem.* **279,** 39414–39420
11. DeFronzo, R. A., and Goodman, A. M. (1995) Efficacy of metformin in patients with non-insulin-dependent diabetes mellitus. The Multicenter Metformin Study Group. *N. Engl. J. Med.* **333,** 541–549
12. Stumvoll, M., Nurjhan, N., Perriello, G., Dailey, G., and Gerich, J. E. (1995) Metabolic effects of metformin in non-insulin-dependent diabetes mellitus. *N. Engl. J. Med.* **333,** 550–554
13. Hundal, R. S., Krssak, M., Dufour, S., Laurent, D., Lebon, V., Chandramouli, V., Inzucchi, S. E., Schumann, W. C., Petersen, K. F., Landau, B. R., and Shulman, G. I. (2000) Mechanism by which metformin reduces glucose production in type 2 diabetes. *Diabetes* **49,** 2063–2069
14. Yang, Y., Shang, W., Zhou, L., Jiang, B., Jin, H., and Chen, M. (2007) Emodin with PPARγ ligand-binding activity promotes adipocyte differentiation and increases glucose uptake in 3T3-Ll cells. *Biochem. Biophys. Res. Commun.* **353,** 225–230
15. Wang, C. H., Gao, Z. Q., Ye, B., Cai, J. T., Xie, C. G., Qian, K. D., and Du, Q. (2007) Effect of emodin on pancreatic fibrosis in rats. *World J. Gastroenterol.* **13,** 378–382
16. Imanishi, Y., Maeda, N., Otogawa, K., Seki, S., Matsui, H., Kawada, N., and Arakawa, T. (2004) Herb medicine Inchin-ko-to (TJ-135) regulates PDGF-BB-dependent signaling pathways of hepatic stellate cells in primary culture and attenuates development of liver fibrosis induced by thioacetamide administration in rats. *J. Hepatol.* **41,** 242–250
17. Yea, K., Kim, J., Lim, S., Park, H. S., Park, K. S., Suh, P. G., and Ryu, S. H. (2008) Lysophosphatidic acid regulates blood glucose by stimulating myotube and adipocyte glucose uptake. *J. Mol. Med.* **86,** 211–220
18. Mu, J., Brozinick, J. T., Jr., Valladares, O., Bucan, M., and Birnbaum, M. J. (2001) A role for AMP-activated protein kinase in contraction- and hypoxia-regulated glucose transport in skeletal muscle. *Mol. Cell* **7,** 1085–1094
19. Zong, H., Ren, J. M., Young, L. H., Pypaert, M., Mu, J., Birnbaum, M. J., and Shulman, G. I. (2002) AMP kinase is required for mitochondrial biogenesis in skeletal muscle in response to chronic energy deprivation. *Proc. Natl. Acad. Sci. U.S.A.* **99,** 15983–15987
20. Kandror, K. V. (2003) A long search for Glut4 activation. *Sci. STKE 2003,* PE5
21. Somwar, R., Perreault, M., Kapur, S., Taha, C., Sweeney, G., Ramlal, T., Kim, D. Y., Keen, J., Côte, C. H., Klip, A., and Marette, A. (2000) Activation of p38 mitogen-activated protein kinase α and β by insulin and contraction in rat skeletal muscle. Potential role in the stimulation of glucose transport. *Diabetes* **49,** 1794–1800
22. Yi, J., Yang, J., He, R., Gao, F., Sang, H., Tang, X., and Ye, R. D. (2004) Emodin enhances arsenic trioxide-induced apoptosis via generation of reactive oxygen species and inhibition of survival signaling. *Cancer Res.* **64,** 108–116
23. Choi, S. L., Kim, S. J., Lee, K. T., Kim, J., Mu, J., Birnbaum, M. J., Soo Kim, S., and Ha, J. (2001) The regulation of AMP-activated protein kinase by H_2O_2. *Biochem. Biophys. Res. Commun.* **287,** 92–97
24. Park, I. J., Lee, Y. K., Hwang, J. T., Kwon, D. Y., Ha, J., and Park, O. J. (2009) Green tea catechin controls apoptosis in colon cancer cells by attenuation of H_2O_2-stimulated COX-2 expression via the AMPK signaling pathway at low-dose H_2O_2. *Ann. N.Y. Acad. Sci.* **1171,** 538–544
25. Zmijewski, J. W., Banerjee, S., Bae, H., Friggeri, A., Lazarowski, E. R., and Abraham, E. (2010) Exposure to hydrogen peroxide induces oxidation and activation of AMP-activated protein kinase. *J. Biol. Chem.* **285,** 33154–33164
26. Hattori, A., Mawatari, K., Tsuzuki, S., Yoshioka, E., Toda, S., Yoshida, M., Yasui, S., Furukawa, H., Morishima, M., Ono, K., Ohnishi, T., Nakano, M., Harada, N., Takahashi, A., and Nakaya, Y. (2010) β-Adrenergic-AMPK pathway phosphorylates acetyl-CoA carboxylase in a high-epinephrine rat model, SPORTS. *Obesity* **18,** 48–54
27. Lumeng, C. N., and Saltiel, A. R. (2011) Inflammatory links between obesity and metabolic disease. *J. Clin. Invest.* **121,** 2111–2117
28. Cha, T. L., Qiu, L., Chen, C. T., Wen, Y., and Hung, M. C. (2005) Emodin down-regulates androgen receptor and inhibits prostate cancer cell growth. *Cancer Res.* **65,** 2287–2295
29. Su, Y. T., Chang, H. L., Shyue, S. K., and Hsu, S. L. (2005) Emodin induces apoptosis in human lung adenocarcinoma cells through a reactive oxygen species-dependent mitochondrial signaling pathway. *Biochem. Pharmacol.* **70,** 229–241
30. Kumar, A., Dhawan, S., and Aggarwal, B. B. (1998) Emodin (3-methyl-1,6,8-trihydroxyanthraquinone) inhibits TNF-induced NF-κB activation, IκB degradation, and expression of cell surface adhesion proteins in human vascular endothelial cells. *Oncogene* **17,** 913–918
31. Liu, Y. X., Shen, N. Y., Liu, C., and Lv, Y. (2009) Immunosuppressive effects of emodin. An *in vivo* and *in vitro* study. *Transplant. Proc.* **41,** 1837–1839
32. Jahnke, G. D., Price, C. J., Marr, M. C., Myers, C. B., and George, J. D. (2004) Developmental toxicity evaluation of emodin in rats and mice. *Birth Defects Res. B. Dev. Reprod. Toxicol.* **71,** 89–101
33. Oshida, K., Hirakata, M., Maeda, A., Miyoshi, T., and Miyamoto, Y. (2011) Toxicological effect of emodin in mouse testicular gene expression profile. *J. Appl. Toxicol.* **31,** 790–800

34. Owen, M. R., Doran, E., and Halestrap, A. P. (2000) Evidence that metformin exerts its anti-diabetic effects through inhibition of complex 1 of the mitochondrial respiratory chain. *Biochem. J.* **348,** 607–614
35. Lenaz, G., Fato, R., Genova, M. L., Bergamini, C., Bianchi, C., and Biondi, A. (2006) Mitochondrial complex I. Structural and functional aspects. *Biochim. Biophys. Acta* **1757,** 1406–1420
36. Feng, Y., Huang, S. L., Dou, W., Zhang, S., Chen, J. H., Shen, Y., Shen, J. H., and Leng, Y. (2010) Emodin, a natural product, selectively inhibits 11β-hydroxysteroid dehydrogenase type 1 and ameliorates metabolic disorder in diet-induced obese mice. *Br. J. Pharmacol.* **161,** 113–126
37. Sandeep, T. C., Andrew, R., Homer, N. Z., Andrews, R. C., Smith, K., and Walker, B. R. (2005) Increased *in vivo* regeneration of cortisol in adipose tissue in human obesity and effects of the 11β-hydroxysteroid dehydrogenase type 1 inhibitor carbenoxolone. *Diabetes* **54,** 872–879
38. Zurlo, F., Larson, K., Bogardus, C., and Ravussin, E. (1990) Skeletal muscle metabolism is a major determinant of resting energy expenditure. *J. Clin. Invest.* **86,** 1423–1427
39. Lee, Y. S., Kim, W. S., Kim, K. H., Yoon, M. J., Cho, H. J., Shen, Y., Ye, J. M., Lee, C. H., Oh, W. K., Kim, C. T., Hohnen-Behrens, C., Gosby, A., Kraegen, E. W., James, D. E., and Kim, J. B. (2006) Berberine, a natural plant product, activates AMP-activated protein kinase with beneficial metabolic effects in diabetic and insulin-resistant states. *Diabetes* **55,** 2256–2264
40. Watt, M. J., Dzamko, N., Thomas, W. G., Rose-John, S., Ernst, M., Carling, D., Kemp, B. E., Febbraio, M. A., and Steinberg, G. R. (2006) CNTF reverses obesity-induced insulin resistance by activating skeletal muscle AMPK. *Nat. Med.* **12,** 541–548
41. Tzeng, T. F., Lu, H. J., Liou, S. S., Chang, C. J., and Liu, I. M. (2012) Emodin, a naturally occurring anthraquinone derivative, ameliorates dyslipidemia by activating AMP-activated protein kinase in high-fat-diet-fed rats. *Evid. Based Complement. Alternat. Med.* **2012**, 781812
42. Tzeng, T. F., Lu, H. J., Liou, S. S., Chang, C. J., and Liu, I. M. (2012) Emodin protects against high-fat diet-induced obesity via regulation of AMP-activated protein kinase pathways in white adipose tissue. *Planta Med.* **78,** 943–950
43. Katz, A. (2007) Modulation of glucose transport in skeletal muscle by reactive oxygen species. *J. Appl. Physiol.* **102,** 1671–1676
44. Loh, K., Deng, H., Fukushima, A., Cai, X., Boivin, B., Galic, S., Bruce, C., Shields, B. J., Skiba, B., Ooms, L. M., Stepto, N., Wu, B., Mitchell, C. A., Tonks, N. K., Watt, M. J., Febbraio, M. A., Crack, P. J., Andrikopoulos, S., and Tiganis, T. (2009) Reactive oxygen species enhance insulin sensitivity. *Cell Metab.* **10,** 260–272
45. Leslie, N. R., Bennett, D., Lindsay, Y. E., Stewart, H., Gray, A., and Downes, C. P. (2003) Redox regulation of PI 3-kinase signaling via inactivation of PTEN. *EMBO J.* **22,** 5501–5510
46. An, Z., Wang, H., Song, P., Zhang, M., Geng, X., and Zou, M. H. (2007) Nicotine-induced activation of AMP-activated protein kinase inhibits fatty acid synthase in 3T3L1 adipocytes. A role for oxidant stress. *J. Biol. Chem.* **282,** 26793–26801
47. Choi, H. C., Song, P., Xie, Z., Wu, Y., Xu, J., Zhang, M., Dong, Y., Wang, S., Lau, K., and Zou, M. H. (2008) Reactive nitrogen species is required for the activation of the AMP-activated protein kinase by statin *in vivo*. *J. Biol. Chem.* **283,** 20186–20197
48. Merry, T. L., and McConell, G. K. (2009) Skeletal muscle glucose uptake during exercise. A focus on reactive oxygen species and nitric oxide signaling. *IUBMB Life* **61,** 479–484
49. Sandström, M. E., Zhang, S. J., Bruton, J., Silva, J. P., Reid, M. B., Westerblad, H., and Katz, A. (2006) Role of reactive oxygen species in contraction-mediated glucose transport in mouse skeletal muscle. *J. Physiol.* **575,** 251–262
50. Collins, Q. F., Liu, H. Y., Pi, J., Liu, Z., Quon, M. J., and Cao, W. (2007) Epigallocatechin-3-gallate (EGCG), a green tea polyphenol, suppresses hepatic gluconeogenesis through 5′-AMP-activated protein kinase. *J. Biol. Chem.* **282,** 30143–30149
51. Fujita, Y., Hosokawa, M., Fujimoto, S., Mukai, E., Abudukadier, A., Obara, A., Ogura, M., Nakamura, Y., Toyoda, K., Nagashima, K., Seino, Y., and Inagaki, N. (2010) Metformin suppresses hepatic gluconeogenesis and lowers fasting blood glucose levels through reactive nitrogen species in mice. *Diabetologia* **53,** 1472–1481
52. Ross, R. M., Wadley, G. D., Clark, M. G., Rattigan, S., and McConell, G. K. (2007) Local nitric oxide synthase inhibition reduces skeletal muscle glucose uptake but not capillary blood flow during *in situ* muscle contraction in rats. *Diabetes* **56,** 2885–2892
53. Shaw, R. J., Lamia, K. A., Vasquez, D., Koo, S. H., Bardeesy, N., Depinho, R. A., Montminy, M., and Cantley, L. C. (2005) The kinase LKB1 mediates glucose homeostasis in liver and therapeutic effects of metformin. *Science* **310,** 1642–1646